

 Open access • Journal Article • DOI:10.1007/S11012-005-3352-Y

Marangoni mixed convection boundary layer flow — Source link

Ali J. Chamkha, Ioan Pop, Harmindar S. Takhar





Institutions: The Public Authority for Applied Education and Training, Manchester Metropolitan University

Published on: 01 Apr 2006 - Meccanica (Kluwer Academic Publishers)

Topics: Marangoni effect, Marangoni number, Boundary layer thickness, Blasius boundary layer and Rayleigh–Bénard convection

Related papers:

- [Exact analytical results for the thermosolutal MHD Marangoni boundary layers](#)
- [Thermosolutal marangoni forced convection boundary layers](#)
- [Non isobaric boundary layers related to Marangoni flows](#)
- [Similarity solutions for MHD thermosolutal Marangoni convection over a flat surface in the presence of heat generation or absorption effects](#)
- [Prandtl number effects for Marangoni convection over a flat surface](#)

Share this paper:    

View more about this paper here: <https://typeset.io/papers/marangoni-mixed-convection-boundary-layer-flow-jpr8fjxdaf>

Marangoni Mixed Convection Boundary Layer Flow

A. J. CHAMKHA, I. POP¹ and H. S. TAKHAR^{2,*}

*Manufacturing Engineering Department, The Public Authority for Applied Education and Training, Shuweikh, 70654, Kuwait;*¹*Faculty of Mathematics, University of Cluj, R-3400 Cluj, CP 253, Romania;*²*Department of Engineering, Manchester Metropolitan University, Manchester M1 5GD, U.K.*

(Received: 29 January 2004; accepted in revised form: 24 August 2005)

Abstract. The paper deals with a steady coupled dissipative layer, called Marangoni mixed convection boundary layer, which can be formed along the interface of two immiscible fluids, in surface driven flows. The mixed convection boundary layer is generated when besides the Marangoni effects there are also buoyancy effects due to gravity and external pressure gradient effects. We shall use a model proposed by Golia and Viviani (*L' Aerotecnica missili e Spazio* **64** (1985) 29–35, *Meccanica* **21** (1986) 200–204) wherein the Marangoni coupling condition has been included into the boundary conditions at the interface. The similarity equations are first determined, and the pertinent equations are solved numerically for some values of the governing parameters and the features of the flow and temperature fields as well as the interface velocity and heat transfer at the interface are analysed and discussed.

Key words: Coupled Marangoni boundary layer, Combined convection, Numerical solution, Immiscible fluids, Fluid mechanics.

1. Introduction

The free surface of a viscous fluid is a source of convective flow, often called Marangoni convection, if its surface tension is distributed non-uniformly (Thess *et al.* [16]). Such a non-uniformity arises from the dependence of the surface tension on a scalar quantity, either surfactant concentration or temperature. An indispensable prerequisite for Marangoni convection is the dependence of the surface tension σ on a scalar field ϕ , which can be the temperature, concentration or a combination of both.

The existence of the steady dissipative layers along the liquid–liquid or liquid–gas interfaces seem to have been first observed by Napolitano [5–7] and were called Marangoni boundary layers or dissipative layers. These layers may exist on both sides of a Marangoni interface, if the non-dimensional Reynolds, Re , and Péclet, Pe , numbers are much larger than one. Since Re and Pe increase with the reference length (i.e. the extension of the interface), in microgravity environment conditions may easily exist to establish a boundary layer regime, contrary to what will happen on Earth (see Golia and Viviani [4]). Problems of this type

*Author for Correspondence: e-mail: h.s.takhar@mmu.ac.uk

are of great importance due to their relevance in several fields of microgravity sciences and space processing. Studies of these problems are also motivated by their importance in terrestrial materials processing, and oceanography (see Skarda *et al.* [14]). The surface tension gradients that are responsible for Marangoni convection can be due to gradients of temperature and/or concentration (thermal/or surfactant concentration). The significance of dissipative layers in liquid metal and semiconductor processing is shown to be particularly strong and is a major factor in guiding the control of industrial processes. However, although much progress has been made, especially in the study of the Marangoni convection, the state of the art is still somewhat unsatisfactory, concerning questions of general and basic nature.

It was shown by Napolitano [7] that, as in the classical steady boundary layers (non-Marangoni layers), the field equations in the bulk fluids do not depend explicitly on the geometry of the interface when using as coordinates the arc length (X) and the distance normal to the interface. This involves however the mean curvature of its hydrostatic and dynamic shapes and, together with the other surface balance equations, introduces kinematic, thermal and pressure couplings for the flow fields in the two fluids. Napolitano and Golia [8] have shown that the fields are uncoupled when the momentum and energy resistance ratios of the two layers and the viscosity ratio of the two fluids are much less than one. Similarly solutions of the steady Marangoni boundary layers exist when the interface temperature gradient varies as a power of the interface arc length (X). The power laws for all other variables, including the mean curvature, were determined. Numerical solutions were found, analyzed and discussed for steady Marangoni boundary layers in some papers by Napolitano and Russo [9], Golia and Viviani [3, 4], Napolitano *et al.* [10, 11], Christopher and Wang [2], and Pop *et al.* [13]. On the other hand, Zeng *et al.* [17–20] have analyzed very recently in a series of papers the oscillatory Marangoni convection under microgravity by assuming that σ decreases linearly with temperature. However, the Marangoni coupling condition has been included in the Navier-Stokes equations and in the boundary conditions at the interface.

The present paper aims to study the steady boundary layers that can be formed along the interface of two immiscible fluids in surface driven flows that may be generated when beside the Marangoni effects there are also buoyancy effects present due to gravity and external pressure gradient. The corresponding similarity equations are then solved numerically for some values of these parameters using a finite-difference method proposed by Blottner [1]. The velocity and temperature profiles as well as the interface velocity and heat transfer at the interface are obtained and discussed.

2. Basic Equations

Consider the steady coupled problem of thermal Marangoni boundary layer with buoyancy effects due to gravity and an external pressure gradient which occurs along an interface S of two immiscible fluids, as shown in Figure 1. It is assumed that the gravity vector \mathbf{g} is aligned with the fluid interface S and that the flow fields of the two interfacing fluids are uncoupled. It is also assumed that the component normal

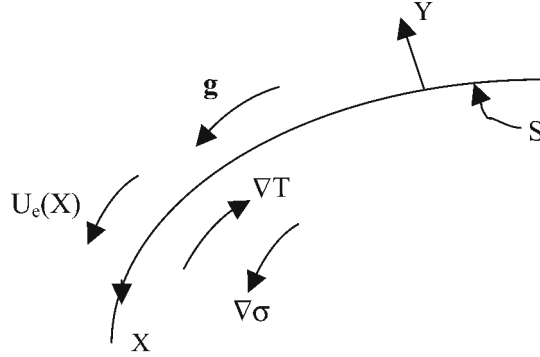


Figure 1. Physical model with interface conditions and coordinate system.

to the interface of the gravity vector \mathbf{g} is neglected, so that the curvature of the interface can be ignored. Under these assumptions, along with the Boussinesq approximation, and neglecting the viscous dissipation, the basic equations for the coupled Marangoni boundary layer are those derived by Golia and Viviani [3, 4], viz

$$\frac{\partial U}{\partial X} + \frac{\partial V}{\partial Y} = 0, \quad (1)$$

$$U \frac{\partial U}{\partial X} + V \frac{\partial U}{\partial Y} = U_e \frac{dU_e}{dX} + \nu \frac{\partial^2 U}{\partial Y^2} - \Gamma g \beta (T - T_m), \quad (2)$$

$$U \frac{\partial T}{\partial X} + V \frac{\partial T}{\partial Y} = \frac{\nu}{Pr} \frac{\partial^2 T}{\partial Y^2}, \quad (3)$$

subject to the boundary conditions

$$\begin{aligned} V &= 0, \quad T = T_S(X) \quad \text{at} \quad Y = 0, \\ U &\rightarrow U_e(X), \quad T \rightarrow T_m \quad \text{as} \quad Y \rightarrow \infty \end{aligned} \quad (4)$$

and the interface condition

$$\mu \frac{\partial U}{\partial Y} = \sigma_T \frac{\partial T}{\partial X}. \quad (5)$$

Here X and Y are the Cartesian coordinates along and normal to the interface S , respectively, U and V are the velocity components parallel to the X and Y axes, $U_e(X)$ is the velocity outside boundary layer, g is the magnitude of the acceleration due to gravity, β is the coefficient of thermal expansion, μ is the dynamic viscosity, ν is the kinematic viscosity, Pr is the Prandtl number and the parameter Γ assumes the values of $\Gamma = \mp 1$ according as the buoyancy forces are favourable to the Marangoni flow ($\Gamma = -1$) or the buoyancy forces are opposing to the Marangoni flow ($\Gamma = +1$), respectively. Further $\sigma_T = -d\sigma/dX > 0$ where σ is the surface tension which is assumed to be given by the linear relation

$$\sigma = \sigma_m - \sigma_T (T - T_m), \quad (6)$$

where σ_m is the surface tension at a reference temperature T_m ; both σ_m and T_m are constants.

The interface condition (5) can be obtained as follows. If t^i and t_{ij} ($i, j = 1, 2, 3$) denote the stress vector and stress tensor, then we have (see Straughan [15])

$$t^i = t_{ij} n_j = \sigma b_\alpha^\alpha n^i + x_{;\alpha} a^{\alpha\gamma} \sigma_{;\gamma} \quad (7)$$

where b_α^α is the mean curvature of the surface, $x_{;\alpha}$ are tangential vectors, $a^{\alpha\gamma}$ is the first fundamental form of the surface, α denotes covariant differentiation with respect to the surface coordinates and n^i are the components of the outward unit normal to the interface. Since

$$t_{ij} = -p \delta_{ij} + 2\mu d_{ij}, \quad d_{ij} = \frac{1}{2} (u_{i,j} + u_{j,i}), \quad (8)$$

where p is the pressure and δ_{ij} is the Kronecker delta operator, relations (7) and (8) give rise to the condition (5) for the component along the interface ($i = 1$). Although there are instances in which relation (5) is inappropriate (see, e.g. Oron and Rosenau [12]), the majority of phenomena in Marangoni convection can be understood in the framework of this simple relation.

We now introduce the following non-dimensional variables

$$\begin{aligned} x &= (X - L_0)/L, & y &= Re^{1/3} (Y/L), & u &= U/U_r, & v &= Re^{1/3} (V/U_r) \\ u_e(x) &= U_e(X)/U_r, & t &= (T - T_m)/\Delta T, & U_r &= Re^{-1/3} U_m, & U_m &= \sigma_T \Delta T/\mu, \end{aligned} \quad (9)$$

where L_0 determines the location of the origin of the curvilinear axis X , Y is the extension of the interface S , ΔT is a positive temperature increment along the interface (relative to the temperature gradient imposed along S), U_m is the Marangoni velocity, U_r is the reference velocity based upon U_m and $Re = U_m L/\nu$ is the Reynolds number based on the Marangoni velocity U_m .

Substituting (9) into equations (1)–(3), we obtain

$$\frac{\partial u}{\partial x} + \frac{\partial v}{\partial y} = 0, \quad (10)$$

$$u \frac{\partial u}{\partial x} + v \frac{\partial u}{\partial y} = u_e \frac{du_e}{dx} + \frac{\partial^2 u}{\partial y^2} - \Gamma \lambda t, \quad (11)$$

$$u \frac{\partial t}{\partial x} + v \frac{\partial t}{\partial y} = \frac{1}{Pr} \frac{\partial^2 t}{\partial y^2} \quad (12)$$

and the boundary conditions (4) reduce to

$$\begin{aligned} \frac{\partial u}{\partial y} &= \frac{\partial t}{\partial x}, & v &= 0, & t &= t_S(x) & \text{at } y &= 0 \\ u &\rightarrow u_e(x), & t &\rightarrow 0 & \text{as } y &\rightarrow \infty, \end{aligned} \quad (13)$$

where, $\lambda \geq 0$ is the Marangoni mixed convection parameter, which is defined as

$$\lambda = g\beta \Delta T L/U_r^2. \quad (14)$$

We notice that $\lambda = 0$ corresponds to the case of Marangoni forced convection flow, which has been studied by Golia and Viviani [4]. We assume now that equations

(10)–(12) subject to the boundary conditions (13) have the following similarity solution

$$\begin{aligned} u &= u_0 x^m f'(\eta), & v &= -u_0 l_0 x^{m-p-1} [(m-p)f(\eta) + p\eta f'(\eta)] \\ t &= -t_0 x^n \theta(\eta), & \eta &= x^p (y/l_0), & u_e(x) &= u_0 x^m \end{aligned} \quad (15)$$

where m , n , p are constants and primes denote differentiation with respect to η , and u_0 , l_0 , t_0 are constant scale factors to be determined. If the variables (15) are substituted into equations (11) and (12), and using also the boundary conditions (13), we obtain $m=3$, $n=5$ and $p=1$. Thus, we have

$$u = u_0 x^3 f'(\eta), \quad v = -u_0 \ell_o (2f + \eta f'), \quad t = -t_0 x^5 \theta(\eta), \quad \eta = x(y/\ell_o). \quad (16)$$

This solution gives $t_S(x) = -t_0 x^5$ for the non-dimensional interface temperature distribution, where the minus sign is due to the orientation of the X -axis that is along the direction of decreasing temperature (we have assumed that ΔT and σ_T are positive).

Using relations (16) in equations (11) and (12), we get the following ordinary differential equations

$$f''' + f f'' + \frac{3}{2}(1 - f'^2) + \Gamma \lambda \theta = 0, \quad (17)$$

$$\theta'' + Pr \left(f \theta' - \frac{5}{2} f' \theta \right) = 0, \quad (18)$$

subject to the boundary conditions (13), which now become

$$\begin{aligned} f(0) &= 0, & f''(0) &= -1, & \theta(0) &= 1, \\ f' &\rightarrow 1, & \theta &\rightarrow 0 \quad \text{as} \quad \eta \rightarrow \infty. \end{aligned} \quad (19)$$

The scale factors u_0 , l_0 and t_0 are chosen in order to simplify the form of equations (17) and (18) as well as the boundary conditions (19) and these have to satisfy the following relations (see Golia and Viviani [3]),

$$u_0 \ell_o^2 = \frac{1}{2}, \quad \frac{t_0 \ell_o^2}{u_0} = 1, \quad \frac{t_0 \ell_o}{u_0} = \frac{1}{5}, \quad (20)$$

which, determine the constants u_0 , ℓ_o and t_0 .

The quantities of physical interest are the velocity component $U(x, y)$ parallel to the interface S , the temperature distribution $T(x, y)$ as well as the interface velocity $U(x, 0)$ and heat transfer at the interface $\frac{\partial T}{\partial y}(x, 0)$, which are given by

$$\begin{aligned} U(x, y) &= U_r^* x^3 f'(\eta), & T(x, y) &= T_m - T_r x^5 \theta(\eta), \\ U(x, 0) &= U_r^* x^3 f'(0), & \frac{\partial T}{\partial y}(x, 0) &= -(T_r/\ell_o) x^5 \theta'(0), \end{aligned} \quad (21)$$

where, U_r^* and ΔT are defined as $U_r^* = u_0 U_r$ and $T_r = t_0 \Delta T$.

3. Results and Discussion

The non-linear system of ordinary differential equations (17) and (18) subject to the boundary conditions (19) has been solved numerically for various values of the Prandtl number $Pr = 0.13, 0.25, 0.5, 0.74, 1.0, 1.5, 2.0, 2.8, 3.0, 3.53, 5.0, 8.0, 10.1, 12.5$

and 15.4 when $\lambda = 0$ (Marangoni forced convection), 1, 2, 4, 6, 8 and 10 using the implicit finite-difference method discussed by Blottner [1]. Both favourable (aiding Marangoni effect, $\Gamma = -1$) and contrary (opposing Marangoni effect, $\Gamma = +1$) flow cases were considered. The equations are discretized using three-point central-difference quotients and, as a consequence, of which a set of algebraic equations results. The algebraic equations are then solved by using the well-known tri-diagonal Thomas algorithm. The computational domain was divided into 196 points and variable step sizes with initial step size of 0.001 and a growth factor of 1.04 were utilised. These step sizes were found to give accurate grid-independent results as verified by the comparison of the reduced interface velocity, $f'(0)$, and the reduced temperature gradient normal to the interface, $-\theta'(0)$, for some values of the Prandtl number Pr when the Marangoni mixed convection parameter $\lambda = 1$ and the pressure gradient is absent ($-dp/dx = u_e(x) \, du_e/dx = 0$) as shown in Table 1. Results obtained by Golia and Viviani [4] using a shooting technique based upon a quasi-linearization algorithm are also included in this table. This method has shown that convergence is not sensitive to the particular choice of the initial guess, thus confirming the good convergence of this method. It is seen that the present results are in very good agreement with those of Golia and Viviani [4]. We are, therefore, confident that the present results are very accurate.

To provide concrete knowledge about the flow and heat transfer characteristics, the numerical results for the reduced velocity $f'(\eta)$ and temperature $\theta(\eta)$ profiles as well as for the interface velocity $f'(0)$ and heat transfer $-\theta'(0)$ are presented

Table 1. Comparison of the values of $f'(0)$ and $-\theta'(0)$ for some values of Pr and $\lambda = 1$ for the Marangoni-buoyant boundary layer case ($u_e du_e/dx = 0$)

Opposing case ($\Gamma = +1$)					Favourable case ($\Gamma = -1$)				
Present			Golia and Viviani [4]		Present			Golia and Viviani [4]	
Pr	$f'(0)$	$-\theta'(0)$	$f'(0)$	$-\theta'(0)$	Pr	$f'(0)$	$-\theta'(0)$	$f'(0)$	$-\theta'(0)$
0.13	1.2311	0.5371	1.230	0.535					
0.25	1.1973	0.7627	1.196	0.762					
0.5	1.1556	1.1064	1.155	1.106					
0.74	1.1301	1.3636	1.130	1.363					
1.0	1.1109	1.5996	1.111	1.599					
1.5	1.0855	1.9799	1.085	1.979	2.8	0.6993	2.0900	0.698	2.087
2.0	1.0686	2.3002	1.068	2.299	3.0	0.7122	2.2095	0.711	2.201
3.53	1.0386	3.0844	1.038	3.084	3.53	0.7349	2.4840	0.734	2.482
5.0	1.0223	3.6860	1.022	3.687	5.0	0.7689	3.1119	0.768	3.109
8.0	1.0031	4.6805	1.003	4.679	8.0	0.8012	4.1199	0.800	4.075
10.1	0.9947	5.2664	0.994	5.265	10.1	0.8137	4.7083	0.813	4.706
12.5	0.9874	5.8651	0.987	5.864	12.5	0.8239	5.3079	0.823	5.305
15.4	0.9810	6.5159	0.981	6.514	15.4	0.8329	5.9598	0.832	5.956

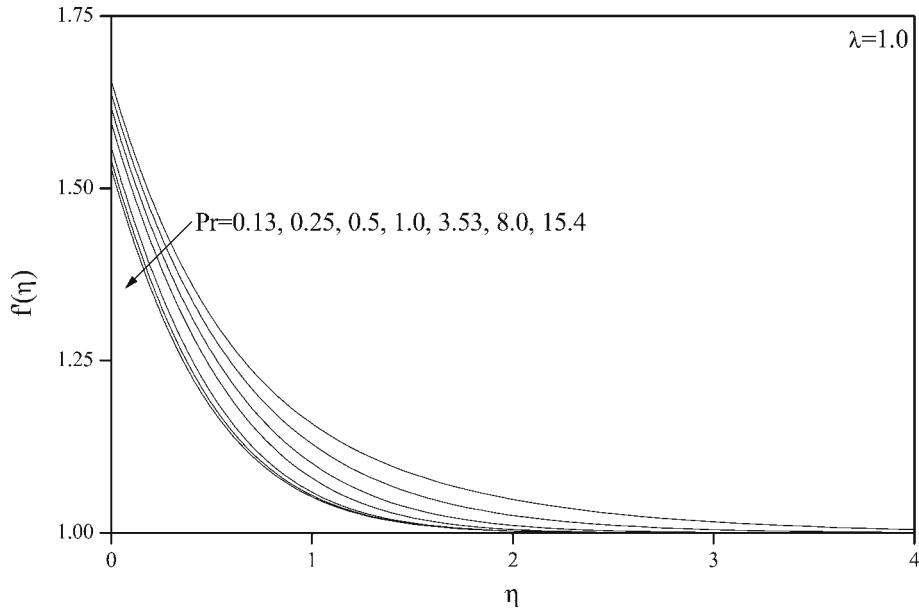


Figure 2. Effects of Pr on velocity profiles for opposing case ($\Gamma = +1$).

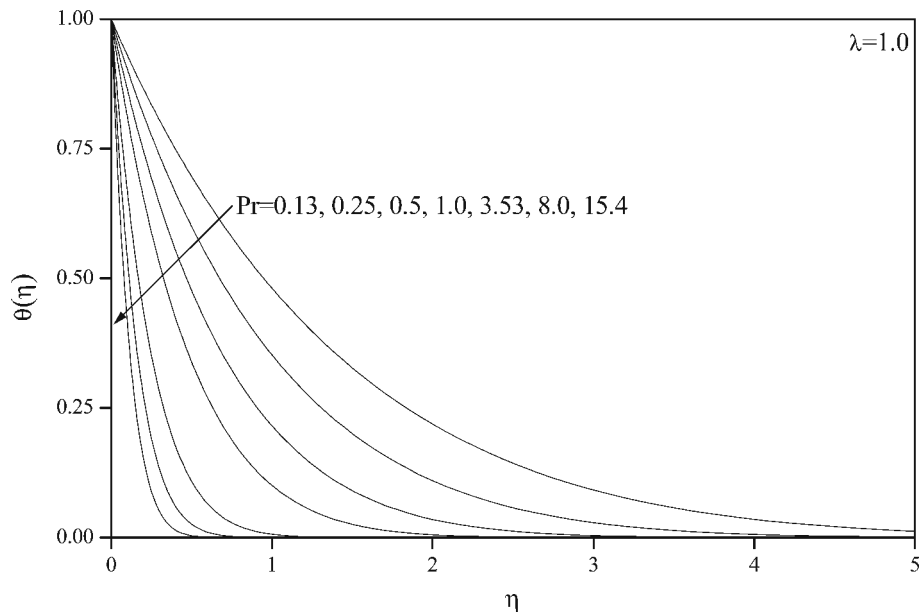


Figure 3. Effects of Pr on temperature profiles for opposing case ($\Gamma = +1$).

in Figures 2–13 for both opposing ($\Gamma = +1$) and favourable ($\Gamma = -1$) cases, respectively. Figures 2–5 show the velocity and temperature profiles for $\lambda = 1$ and some values of the Prandtl number Pr . It is seen that for the opposing case, both the velocity and temperature profiles decrease as Pr increases, while for the favourable case the velocity profiles increase and the temperature profiles decrease with an increase of Pr . However, Figures 3 and 5 show that the temperature profiles are steeper when the flow is opposing and flatter when it is favourable. It should

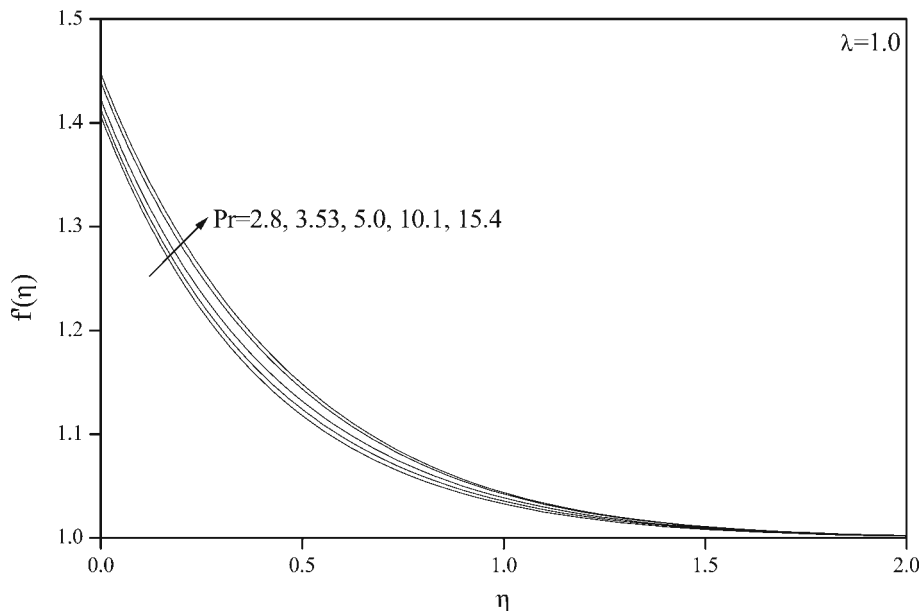


Figure 4. Effects of Pr on velocity profiles for favourable case ($\Gamma = -1$).

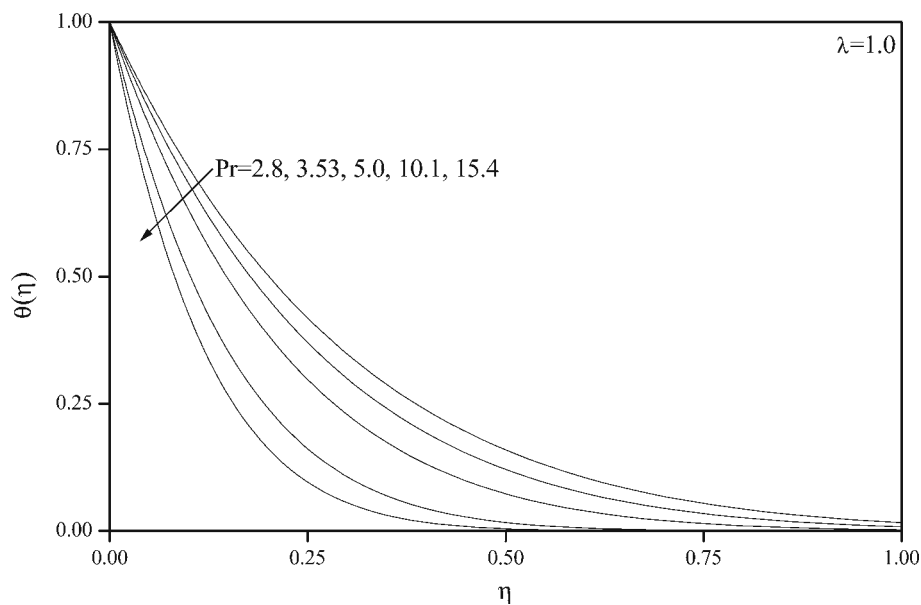


Figure 5. Effects of Pr on temperature profiles for favourable case ($\Gamma = -1$).

also be noticed that in the opposing case, the numerical procedure converges for any value of Pr , whereas in the favourable case, the solution scheme does not converge for Pr less than 2.8. This is in agreement with the results reported by Golia and Viviani [4]. Figures 6–9 represent the variation of the velocity and temperature profiles for $Pr = 3.53$ and several values of λ . It can be noticed from Figures 6 and 8 that the velocity profiles increase for the opposing case ($\Gamma = +1$) while they decrease for the favourable case ($\Gamma = -1$), when the parameter λ increases.

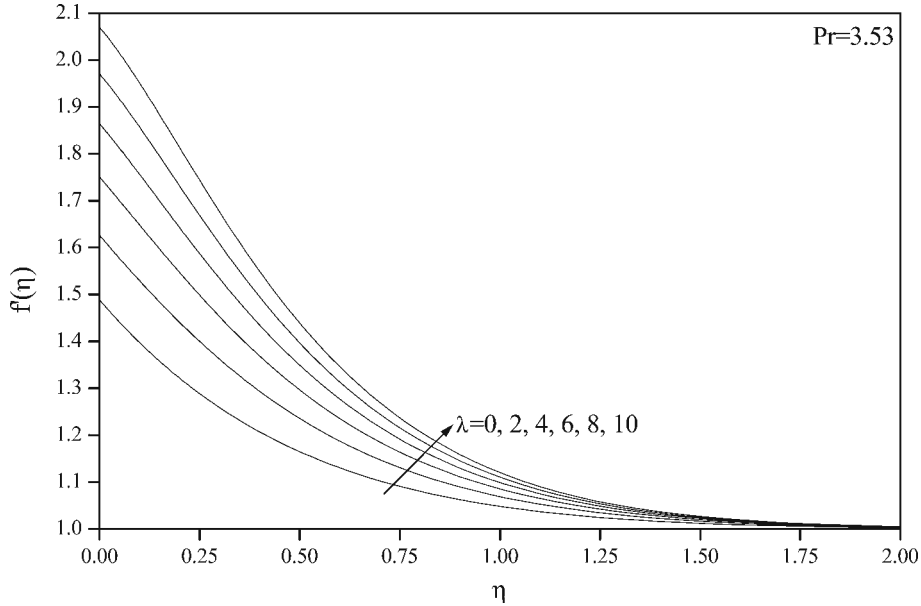


Figure 6. Effects of λ on velocity profiles for opposing case ($\Gamma = +1$).

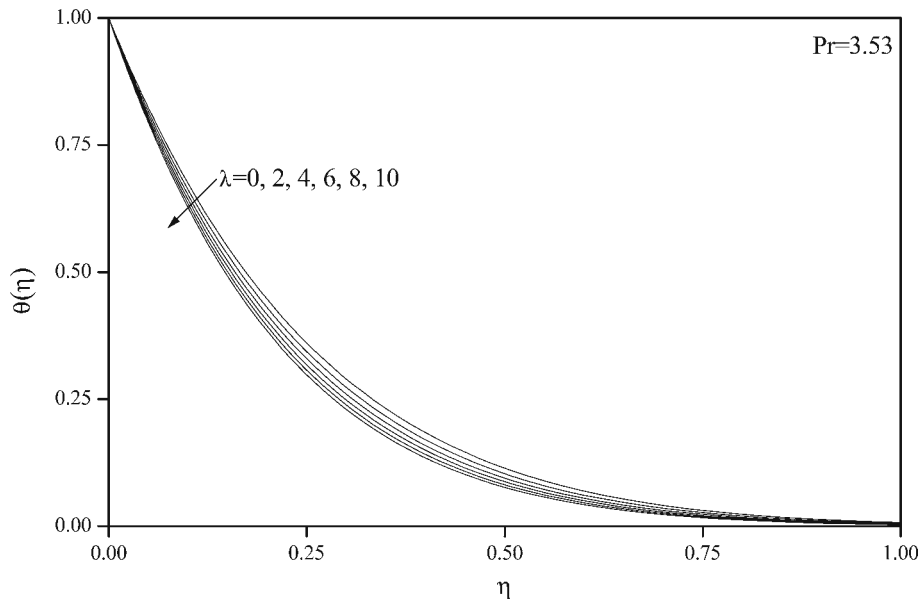


Figure 7. Effects of λ on temperature profiles for opposing case ($\Gamma = +1$).

Furthermore, for the favourable case, these profiles have a minimum close to the interface for λ in the range $4 \leq \lambda \leq 6$, as can be seen from Figure 8. This figure also shows the substantial influence of the buoyancy forces ($\lambda \neq 0$) on the velocity profiles and that these profiles go to one at the end of the boundary layer. On the other hand, the temperature profiles decrease for the opposing flow case and increase for the favourable flow case when λ is increased, as can be

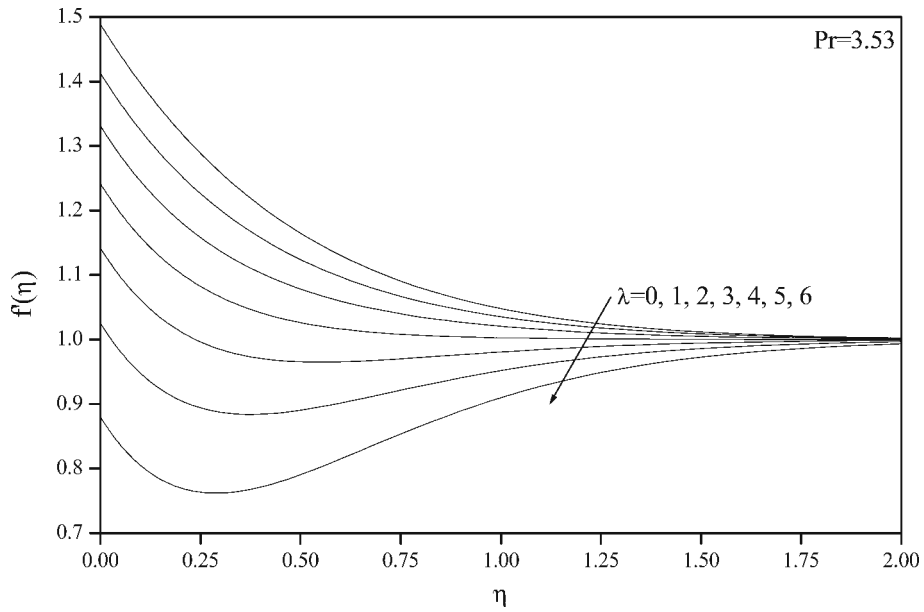


Figure 8. Effects of λ on velocity profiles for favourable case ($\Gamma = -1$).

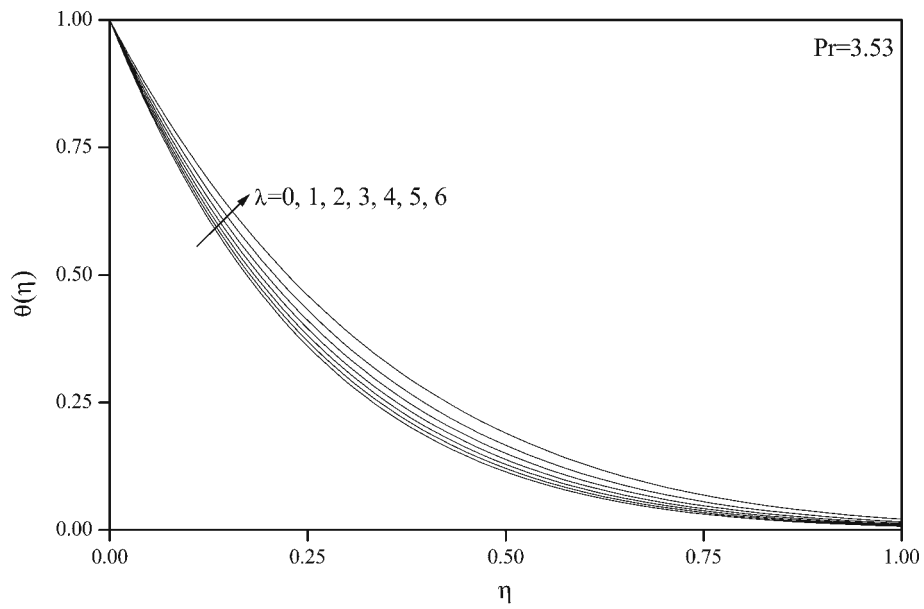


Figure 9. Effects of λ on temperature profiles for favourable case ($\Gamma = -1$).

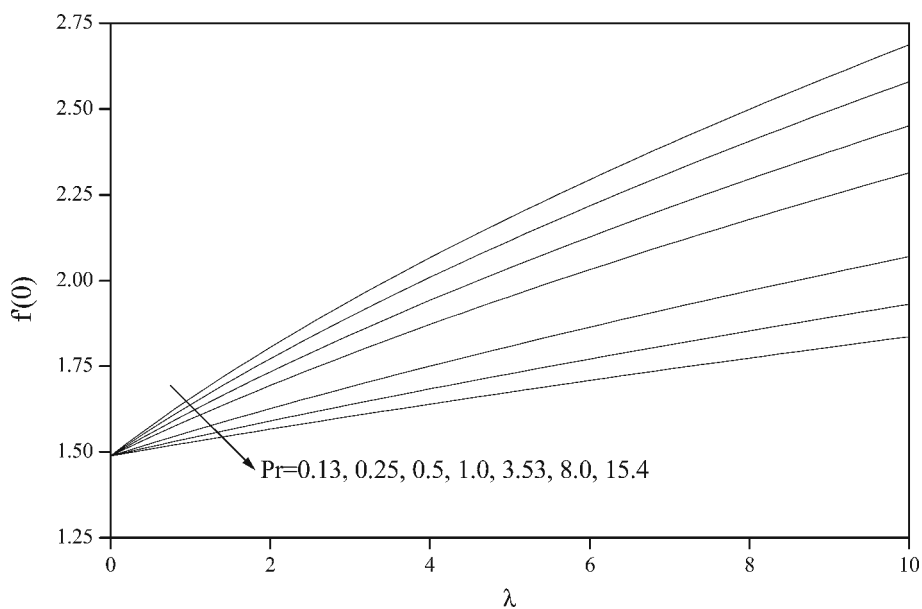


Figure 10. Effects of Pr and λ on the interface velocity for opposing case ($\Gamma = +1$).

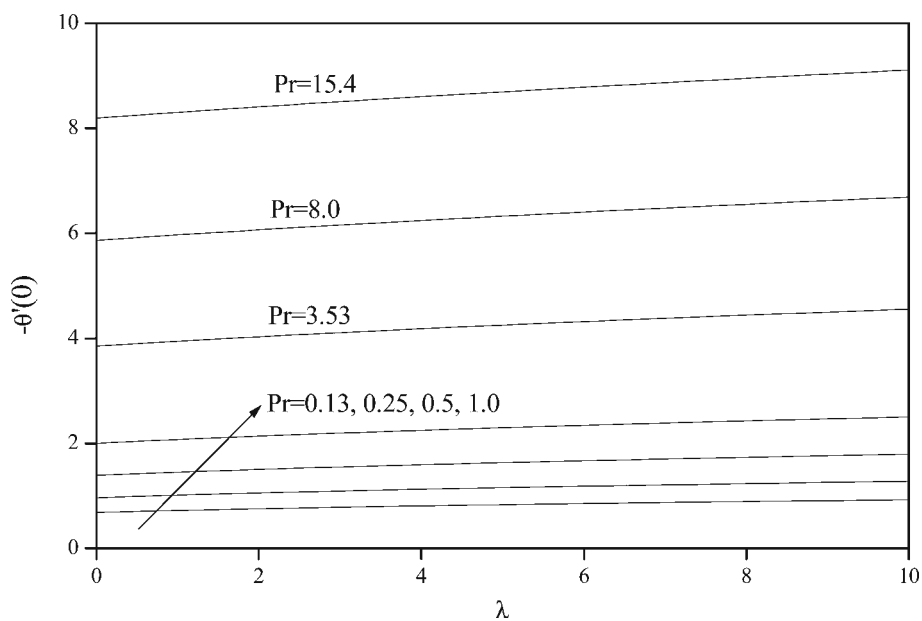


Figure 11. Effects of Pr and λ on the heat flux for opposing case ($\Gamma = +1$).

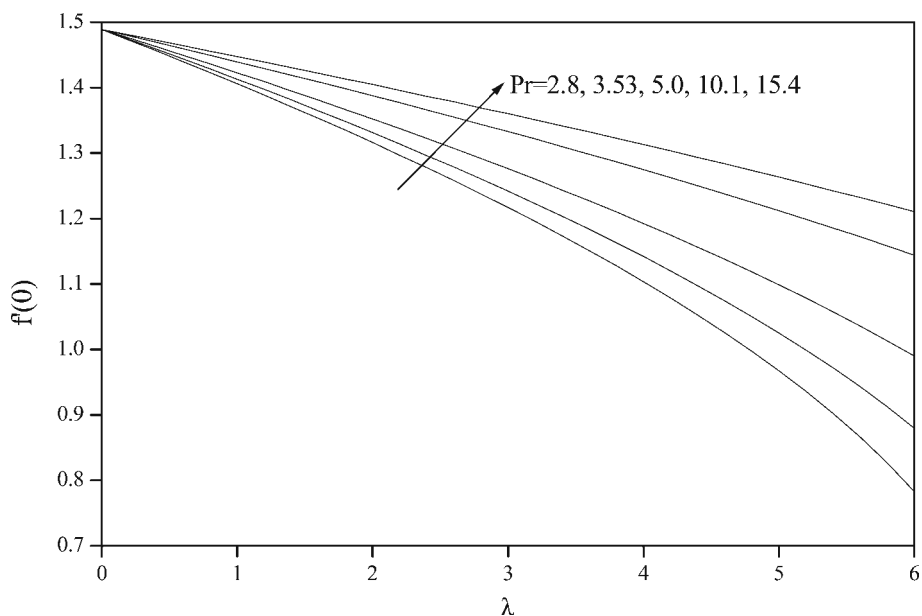


Figure 12. Effects of Pr and λ on the interface velocity for favourable case ($\Gamma = -1$).

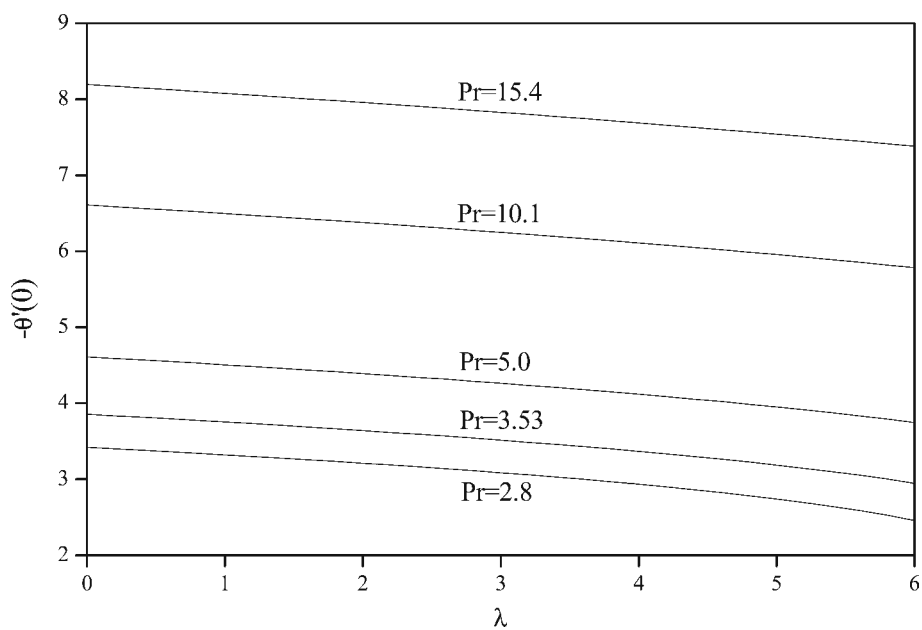


Figure 13. Effects of Pr and λ on the heat flux for favourable case ($\Gamma = -1$).

seen from Figures 7 and 9. All the profiles displayed in Figures 2–7 and 9 tend to zero at the end of the boundary layer, i.e. the thicknesses of the momentum and thermal boundary layers decrease to zero. Finally, Figures 10–13 display the variation with λ of the interface velocity $f'(0)$ and heat transfer at the interface $-\theta'(0)$ for some values of Pr in the range $0.13 \leq Pr \leq 15.4$. One can see that the variation of $f'(0)$ and $-\theta'(0)$ is almost linear with the increase of λ except for $f'(0)$ in the case of favourable flow. It is to be noticed again that the values of $f'(0)$ and $-\theta'(0)$ can be obtained only for $Pr \geq 2.8$ when the Marangoni flow is favourable.

4. Conclusion

A detailed numerical solution is carried out for the steady coupled Marangoni boundary layer flow. The normal component of the gravity vector has been neglected so that the interface curvature has not been considered. This problem differs from that of Golia and Viviani [4] by including the longitudinal pressure gradient term, $-dp/dx = u_e du_e/dx$, into the momentum equation (2), which transforms it into a Marangoni mixed convection boundary layer flow problem. The conditions for the existence of similarity solutions were found and the full boundary layer equations are reduced to similarity or ordinary differential equations. These equations were integrated numerically using a very efficient numerical scheme developed by Blottner [1]. The velocity and temperature profiles as well as the interface velocity and heat transfer at the interface are determined and discussed in detail. It is concluded that the Marangoni mixed convection parameter λ has a substantial effect on the flow and heat transfer characteristics. The contribution of the present study is shown graphically in Figures 2–13. As argued in the Introduction, it is important to know the picture of the Marangoni flow and heat transfer for a large range of values of the parameters λ and Pr because for $\lambda \neq 0$ and some values of Pr this flow model eventually breaks down. More extensive numerical experiments are necessary in an attempt to resolve this situation.

Acknowledgements

The authors wish to express their thanks to the referees for their valuable comments which led to the improvement of the paper.

References

1. Blottner, F. G., 'Finite difference-methods of solutions of the boundary layer equations', *AIAA J.* **8** (1970) 193–205.
2. Christopher, D.M. and Wang, B.-X., 'Similarity solution for Marangoni convection around a vapor bubble during nucleation and growth', *Int. J. Heat Mass Transfer* **44** (2001) 799–810.
3. Golia, C. and Viviani, A., 'Marangoni buoyant boundary layers', *L'Aerotecnica Missili e Spazio* **64** (1985) 29–35.

4. Golia, C. and Viviani, A., 'Non isobaric boundary layers related to Marangoni flows', *Meccanica* **21** (1986) 200–204.
5. Napolitano, L.G., 'Microgravity fluid dynamics', in: *2nd Levitch Conference*, Washington, 1978.
6. Napolitano, L.G., 'Marangoni boundary layers', in: *Proceedings of the 3rd European Symposium on Material Science in Space*, Grenoble, ESA SP-142, June 1979.
7. Napolitano, L.G., 'Surface and buoyancy driven free convection', *Acta Astronautica* **9** (1982) 199–215.
8. Napolitano, L.G. and Golia, C., 'Coupled Marangoni boundary layers', *Acta Astronautica* **8** (1981) 417–434.
9. Napolitano, L.G. and Russo, G., 'Similar axially symmetric Marangoni boundary layers', *Acta Astronautica* **11** (1984) 189–198.
10. Napolitano, L.G., Carlomagno, G.M. and Vigo, P., 'New classes of similar solutions for laminar free convection problems', *Int. J. Heat Mass Transfer* **20** (1977) 215–226.
11. Napolitano, L.G., Viviani, A. and Savino, R., 'Double-diffusive boundary layers along vertical free surfaces', *Int. J. Heat Mass Transfer* **35** (1992) 1003–1025.
12. Oron, A. and Rosenau, P., 'On a nonlinear thermocapillary effect in thin liquid layers', *J. Fluid Mech.* **273**, (1994) 361–374.
13. Pop, I., Postelnicu, A. and Groşan, T., 'Thermosolutal Marangoni forced convection boundary layers', *Meccanica* **36** (2001) 555–571.
14. Skarda, J.R.L., Jacqmin, D. and McCaughan, F.E., 'Exact and approximate solutions to the double-diffusive Marangoni-Bénard problem with cross-diffusive terms', *J. Fluid Mech.* **366** (1998) 109–133.
15. Straughan, B., 'Surface-tension-driven convection in a fluid overlying a porous layer', *J. Comp. Phys.* **170** (2001) 320–337.
16. Thess, A., Spirn, D. and Jüttner, B., 'A two-dimensional model for slow convection at infinite Marangoni number', *J. Fluid Mech.* **331** (1997) 283–312.
17. Zeng, Z., Mizuseki, H., Higashino, K. and Kawazoe, Y., 'Direct numerical simulation of oscillatory Marangoni convection in cylindrical liquid bridges', *J. Crystal Growth* **204** (1999) 395–404.
18. Zeng, Z., Mizuseki, H., Shimamura, K., Higashino, K., Fukuda, T. and Kawazoe, Y., 'Marangoni convection in model of floating zone under microgravity', *J. Crystal Growth* **229** (2001) 601–604.
19. Zeng, Z., Mizuseki, H., Simamura, K., Fukuda, T., Higashino, K. and Kawazoe, Y., 'Three-dimensional oscillatory thermocapillary convection in liquid bridge under microgravity', *Int. J. Heat Mass Transfer* **44** (2001) 3765–3774.
20. Zeng, Z., Mizuseki, H., Shimamura, K., Fukuda, T., Kawazoe, Y. and Higashino, K., 'Usefulness of experiments with model fluid for thermocapillary convection – effect of Prandtl number on two-dimensional thermocapillary', *J. Crystal Growth* **234** (2001) 272–278.